Adaptive Spectral Estimation for Multibaseline SAR Tomography with Airborne L-band Data

Fabrizio Lombardini
Dept. of Information Engineering
University of Pisa, via Diotisalvi 2
56126 Pisa, Italy
f.lombardini@ing.unipi.it

Andreas Reigber
Dept.of Photogrammetry and Cartography
Technical University of Berlin, EB9
10623 Berlin, Germany
anderl@fpk.tu-berlin.de

***Abstract*—In the recent years there has been growing interest in exploiting multibaseline (MB) SAR interferometry in a tomographic framework, to produce full 3D imaging e.g. of forest layers. However, Fourier-based MB SAR tomography is generally affected by unsatisfactory imaging quality due to a typically low number of baselines and their irregular distribution. In this work, we apply the more modern adaptive Capon spectral estimator to the vertical image reconstruction problem, using real airborne MB data. A first demonstration of possible imaging enhancement in real-world conditions is given.**

Keywords- synthetic aperture radar interferometry, electromagnetic tomography, forestry, spectral analysis.

I. INTRODUCTION

SAR systems operating with long (decimetric to metric) radio wavelengths possess the capability of penetrating deep into forest volume, making them an ideal sensor for forest investigations. However, in areas of dense vegetation, the main drawback with current available SAR systems is that efforts to correlate backscattered energy with biomass tend to saturate. A very promising advance in this field is represented by the technique of SAR tomography, which is a multibaseline (MB) extension of conventional SAR interferometry, employing many (on the order of ten) passes over the same area. This produces an aperture synthesis also along the vertical (z) plane to get full 3D imaging [1]. SAR tomography allows direct imaging of semitransparent volume scattering layers and layover surface patches [2] and is, therefore, a promising technique for estimation of biomass, forest and building heights, bald earth topography, and in general improved inversion of geophysical parameters. A first experiment employing MB SAR tomography over forested areas has recently been carried out using the L-band airborne SAR from DLR, successfully demonstrating the concept [3].

However, the current tomographic SAR technique is limited by the typically low number of flight tracks and their irregular distribution, which cannot be avoided under experimental conditions. With conventional tomographic focussing based on Fourier-transforms, an ideal point-spread function cannot be obtained from such data. Especially the irregular sampling causes anomalous side- and grating-lobes of the point-spread function when using a Fourier-based spatial spectral estimation technique.

In this paper, we cast the z-image reconstruction problem in the more modern framework of adaptive spectral estimation. Results obtained by processing real airborne data are reported, proving the adaptive MB processing concept and the resulting imaging enhancement in real-world conditions. In particular, the modern Capon spectral estimator [4] is applied for processing tomographic SAR data with an irregular track distribution, collected over a forested area.

II. CAPON MB SAR TOMOGRAPHY

The Capon method is a non-model based adaptive (data-dependent) filterbank method, originally derived for processing of seismic signals [5]. It can be applied both to time-series analysis and array processing. The shape of its frequency response properly changes during the spectral scan, depending on the input data. In array processing, this allows to adaptively reject interference coming from noise and scattering from other directions than the selected.

In the MB SAR tomography framework, we assume to process the data from a non-uniform cross-track array of K phase centers (see [3]). This is usually synthesized by K repeated flight tracks of a single-channel SAR over the area of interest. After motion compensation, K registered complex SAR images are produced. As usual in SAR imaging and interferometry, in each SAR image we consider N i.i.d. looks to reduce statistical variations, e.g. multiple homogeneous adjacent pixels. For each n-th look, $n=1,...,N$, the complex amplitudes of the pixels observed in the K SAR images at a given range-azimuth cell, are arranged in the $K\times 1$ vector $\mathbf{y}(n)$. Assuming the first phase center as reference (master track), consider the $K\times 1$ steering vector $\mathbf{a}(z)$, coding the cross-track array response to a backscattered signal component coming from height z:

$$\mathbf{a}(z) = [1 \quad e^{j\varphi_2(z)} \quad \dots \quad e^{j\varphi_K(z)}]^T . \qquad (1)$$

Here, $\varphi_i(z) = -(4\pi/\lambda)[d_i(z) - d_1(z)]$ is the interferometric phase between the i-th and the master phase center due to the differential slant-range distance for a point located at height z over the ground, with λ the radar wavelength. Assuming the mean of the tracks locations as a reference, the slant-range distance can be well approximated as

$$d_i(z) = \{[H - z + p_{zi}]^2 + [y + p_{yi} + z/\tan(\vartheta)]^2\}^{1/2},\ i=1,...,K, \quad (2)$$

where H is the height over ground of the reference, p_{zi} and p_{yi} are the i-th track vertical and horizontal displacements from the reference, y is the (z=0) ground-range distance from the reference, and ϑ is the off nadir angle at mid-swath. This expression of $\mathbf{a}(z)$ takes directly into account the non-uniform and non-linear structure of the array, and wavefront curvature.

The problem of the z-image reconstruction for a given range-azimuth cell can be described as the estimation of the backscattered signal power height spectrum $P(z)$ from the MB multilook data $\mathbf{y}(n)$, $n=1,...,N$. By applying the Capon method [4], a set of array re-phasing (spatial filtering) coefficients $\mathbf{h}(z)$ is designed that passes the signal component coming from height z in $\mathbf{y}(n)$ without distortion and, at the same time, attenuates all the other signal components from different heights as much as possible. The resulting spatial filter changes both with z and, notably, with the power height spectrum - thus it is data-adaptive. The produced beam shape changes during the height scan depending on the input data, rejecting interference coming from scattering from other heights than the selected. This allows gains in terms of both resolution and leakage (sidelobe) level [5]. The Capon estimated power z-image is

$$\hat{P}_C(z) = [\mathbf{a}^H(z)\hat{\mathbf{R}}_y^{-1}\mathbf{a}(z)]^{-1} \quad (3)$$

where $(\cdot)^H$ denotes conjugate transpose, and $\hat{\mathbf{R}}_y$ is a multilook estimate of the array data covariance matrix. The scaling to produce a true power spectral density [4] is not included in (3). The matrix inversion process may amplify estimation errors, thus methods to stabilize $\hat{\mathbf{R}}_y$ may be useful. Since the array is not uniform, we resort to the unstructured sample covariance matrix estimate, and include diagonal loading for robustness:

$$\hat{\mathbf{R}}_y = (1-\alpha)N^{-1}\sum_{n=1}^{N}\mathbf{y}(n)\mathbf{y}^H(n) + \alpha(\sigma_v^2 + \sigma_s^2)\mathbf{I}, \quad (4)$$

where α is the loading factor and $\sigma_v^2 + \sigma_s^2 = \sigma_y^2$ is the total signal power, with σ_v^2 the thermal noise power and σ_s^2 the useful signal power. Following [5], we use the variable loading algorithm $\alpha = \sigma_v^2/(\sigma_v^2 + \sigma_s^2)$, to make estimation possible even when the number of looks N is lower than K and the sample covariance matrix would be singular [4]. We implement the variable loading by using the local MB-multilook incoherently averaged image intensity in place of $\sigma_v^2 + \sigma_s^2 = \sigma_y^2$, and the lowest MB-multilook intensity in the scene in place of σ_v^2. In MB tomography, operating with low N can be useful to keep a high horizontal resolution of the produced tomographic map, and if azimuth looks are taken, to keep as constant as possible the array structure over the multilook data set, despite the possible non-straight real flight tracks. It is also known that diagonal loading produces some robustness to errors in the assumed steering vector [6]. In MB tomography, this can be useful since the measured/calibrated tracks displacements p_{zi} and p_{yi}, $i=1,...,K$, can be affected by errors.

III. Experimental Results by Processing Recorded Live Airborne L-band Data

To get a feeling of the achievable results, a sample of simulated Capon tomography is compared with Fourier tomography. We consider a K=5 phase center non-uniform linear array with spatial lags 0, 2, 4, 7 and 8, with respect to the master phase center, obtained by thinning a 9-phase center uniform array. The MB data are generated according to the statistical model in [2] with N=32 looks. The spatial spectrum considered consists of two squared-Sinc shaped components with mainlobe extension of 0.1 and 1, separated by 1.1, in Rayleigh resolution units. The SNR of the two components in isolation is 9 and 12 dB, respectively. This scenario corresponds to two layover surface patches with different slopes, or can roughly represent a thin volume scattering layer above surface/double-bounce scatterers. Three realizations of the Capon estimated z-image (3), without diagonal loading, are shown in Fig. 1, where the abscissas report z in Rayleigh resolution units around a reference point midway the two components. The (unwindowed) Fourier-based tomographic processor considered employs the Beamforming spatial filter $\hat{P}_B(z) = \mathbf{a}^H(z)\hat{\mathbf{R}}_y\mathbf{a}(z)/K^2$ [4], [2]. It is apparent how the Beamforming estimated z-image realizations are strongly affected by anomalous sidelobes because of the non-uniform phase center distribution. Also, the different extension of the two components can hardly be noticed because of the limited resolution. In contrast, the Capon tomographic processor exhibits much better sidelobe behaviour, and the narrower (left) component is better resolved, beyond the Rayleigh limit.

For a first experimental demonstration of the Capon tomographic processor, a L-band data set with VV polarization of the E-SAR system from DLR was used. The E-SAR sensor is equipped with a high-precision real-time navigation system, based on a combination of DGPS and INS. Using this system, complicated track configurations can be realised with a precision of about 5m in the first try. In the frame of a tomographic experiment, 14 parallel tracks with a mutual nominal distance of 20m have been flown over the testsite of Oberpfaffenhofen/Germany [3]. This configuration corresponds to a vertical resolution of about 2.9m in mid-range when Fourier-based tomography is used. First, the acquired raw-data have been focussed using an extended chirp-scaling processor, which includes a high-precision motion-compensation. After focussing, the data have been coregistered to a common geometry. Finally, a phase calibration took place using a single corner-reflector [3]. This is necessary because the absolute precision of the navigation system is limited to 5-10cm, which in L-band corresponds already to a phase error of about 360 deg within the tomographic aperture.

In the following the K=14 track data set was processed with the diagonal-loaded Capon tomographic processor, and again with unwindowed Beamforming. For a fair comparison, also Beamforming was loaded, although the effect for it is negligible. One height/azimuth slice of the results is shown in Figs. 2 and 3 (amplitude image, arbitrary units). N=13 azimuth

looks have been processed. The right part of the scene consists of nearly flat grass land with a corner reflector placed on it. In the middle of the scene, there is a row of parked cars followed by a building. Beyond the building, the azimuth slice crosses some bushes, a street, and then enters a dense spruce forest with a height of 15 to 20 meters [3].

As a result of the strong anomalous sidelobes of the Beamforming point spread function when operating with the actual irregular track distribution (see [3]), the overall image contrast is low. The *z*-image of the corner reflector and of the bulding roof is badly blurred. The cars and forest crown can be seen, but the others scene features are hardly visible. Conversely, in the Capon-processed tomographic slice both the roof and the corner reflector are sharply imaged, the sidelobe artifacts are drastically reduced. Also, the corner reflector is apparently resolved beyond the Rayleigh limit (2.9m). The cars are much better visible. The grassland profile and the bushes are now clearly identifiable. Also the image contrast for the forest crown and the underlying ground is improved, although some sidelobe artifacts are still present here. This may be attributed to the fact that the degrees of freedom for the Capon filter adaptivity are reduced when the spatial spectrum covers almost all the unambiguous height range (which is about 35m). Another reason may be errors in the track positions, which are calibrated to zero over the reflector but are present over the forest, and to which Capon may be more sensitive than Beamforming [6]. Other results, not reported here, also showed the possibility of slightly relaxing the required number of tracks and tomographic aperture with negligible resolution loss when Capon tomography is employed.

IV. CONCLUSIONS

The Capon MB SAR tomography concept has been applied to real airborne L-band data, experimentally showing that application of adaptive spectral estimators to MB SAR tomography can produce a better imaging quality than Fourier methods with a limited and not fully sampled overall baseline. The results presented here are only a first step into this framework, but the technical feasibility of better exploiting the multi-pass data, both in the sense of resolution and sidelobe level, could clearly be demonstrated. The adaptive processing framework may be alternative or complementary to other modern approaches [7]. It may significantly contribute to the advance of SAR tomography, whose possible application as an effective remote sensing technique is expected to increase both exploiting airborne repeat-pass systems, and future spaceborne clusters of mini-satellites for global monitoring.

ACKNOWLEDGMENT

The authors wish to thank Dr. Alberto Moreira from DLR for providing the E-SAR raw data.

REFERENCES

[1] J. Homer, I. D. Longstaff, G. Callaghan, "High resolution 3-D SAR via multi-baseline interferometry," *Proc. 1996 IEEE Int. Geosci. and Remote Sensing Symp.*, pp 796-798, Lincoln, Nebraska, 1996.

[2] F. Lombardini, M. Montanari, F. Gini, "Reflectivity estimation for multibaseline interferometric radar imaging of layover extended sources," *IEEE Trans. on Signal Processing*, vol. 51, no. 6, June 2003.

[3] A. Reigber, A. Moreira, "First demonstration of airborne SAR tomography using multibaseline L-band data," *IEEE Trans. on Geosci. and Remote Sensing*, vol. 38, no. 5, pp. 2142-2152, September 2000.

[4] P. Stoica, R. Moses, Introduction to spectral analysis. N. J.: Prentice Hall, 1997.

[5] J. Capon, "High resolution frequency wavenumber spectrum analysis," *Proc. IEEE*, vol. 57, pp 1408-1418, August 1969.

[6] H.L. Van Trees, Optimum array processing. Part IV of Detection, estimation, and modulation theory. N.Y.: John Wiley & Sons, 2002.

[7] P. Berardino, G. Fornaro, R. Lanari, E. Sansosti, F. Serafino, F. Soldovieri, "Multi-pass synthetic aperture radar for 3-D focusing," *Proc. 2002 IEEE Int. Geosci. and Remote Sensing Symp.*, pp. 176–178, Toronto, Canada, 2002.

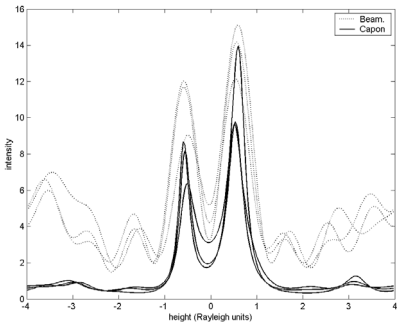

Figure 1. Simulated Beamforming and Capon MB tomographic profiles

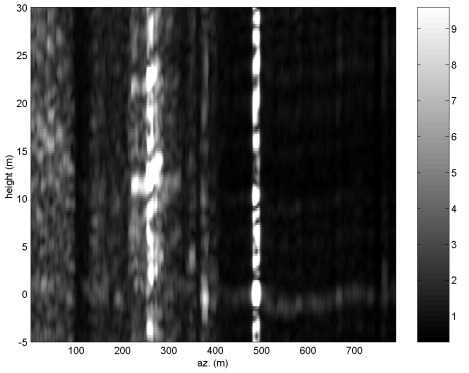

Figure 2. Slice of real Beamforming MB tomography result

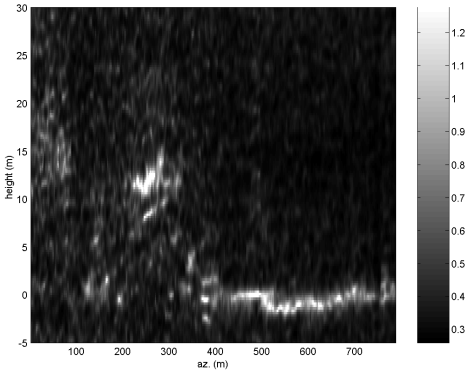

Figure 3. Slice of real Capon MB tomography result